HHS Public Access

Author manuscript

Magn Reson Med. Author manuscript; available in PMC 2024 October 01.

Published in final edited form as:

Magn Reson Med. 2023 October ; 90(4): 1537–1546. doi:10.1002/mrm.29739.

B_1^+ Inhomogeneity Correction of Volumetric Brain NOE_{MTR} via High Permittivity Dielectric Padding at 7T

Paul S Jacobs[1], **Blake Benyard**[1], **Quy Cao**[2], **Anshuman Swain**[1], **Neil Wilson**[1], **Ravi Prakash Reddy Nanga**[1], **M. Dylan Tisdall**[3], **John Detre**[1,4], **Mark A Elliott**[1], **Mohammad Haris**[1], **Ravinder Reddy, PhD**[1]

[1]Center for Advanced Metabolic Imaging in Precision Medicine, Department of Radiology, University of Pennsylvania, Philadelphia, PA, United States

[2]Penn Statistics in Imaging and Visualization Center, Department of Biostatistics, Epidemiology, and Informatics, University of Pennsylvania, Philadelphia, PA, United States

[3]Department of Radiology, University of Pennsylvania, Philadelphia, PA, United States

[4]Department of Neurology, University of Pennsylvania, Philadelphia, PA, United States

Abstract

Purpose: NOE_{MTR} is a technique used to investigate brain lipids and macromolecules in greater detail than other techniques and benefits from increased contrast at 7T. However, this contrast can become degraded due to B_1^+ inhomogeneities present at ultra-high field strengths. High-permittivity dielectric pads (DP) have been used to correct for these inhomogeneities via displacement currents generating secondary magnetic fields. The purpose of this work is to demonstrate that dielectric pads can be used to mitigate B_1^+ inhomogeneities and improve NOE_{MTR} contrast in the temporal lobes at 7T.

Methods: Partial 3D NOE_{MTR} contrast images and whole brain B_1^+ field maps were acquired on a 7T MRI across six healthy subjects. Calcium titanate DP, having a relative permittivity of 110, were placed next to the subject's head near the temporal lobes. Pad corrected NOE_{MTR} images had a separate post-processing linear correction applied.

Results: DP provided supplemental B_1^+ to the temporal lobes while also reducing the B_1^+ magnitude across the posterior and superior regions of the brain. This resulted in a statistically significant increase in NOE_{MTR} contrast in substructures of the temporal lobes both with and without linear correction. The padding also produced a convergence in NOE_{MTR} contrast towards approximately equal mean values.

Conclusion: NOE_{MTR} images showed significant improvement in temporal lobe contrast when DP were used which resulted from an increase in B_1^+ homogeneity across the entire brain slab. DP-derived improvements in NOE_{MTR} are expected to increase the robustness of the brain substructural measures both in healthy and pathological conditions.

Corresponding Author: Ravinder Reddy, PhD, Center for Advanced Metabolic Imaging in Precision Medicine, 422 Curie Boulevard, B1, Stellar Chance Labs, Philadelphia, PA, 19104, krr@pennmedicine.upenn.edu.

Keywords

NOE_{MTR}; Ultra-High Field; Dielectric Padding; B1+ Inhomogeneity Correction

Introduction

Nuclear Overhauser Effect magnetization transfer ratio (NOE_{MTR}) is an emerging MRI technique that has been used to investigate macromolecules in the brain, such as lipids and proteins[1]. This imaging technique takes advantage of magnetization transfer via dipolar cross-relaxation between saturated (lipids and proteins) and unsaturated (bulk water) spin systems, to produce endogenous contrast. Previous studies have demonstrated the application of NOE_{MTR} imaging in mapping the degraded protein content in high-grade brain tumors[2], identifying regional brain damage due to acute ischemic strokes[2], and investigating neurodegenerative disorders such as Parkinson's[3] and Alzheimer's[4]. This gives NOE_{MTR} imaging considerable clinical potential as a significant imaging biomarker for many pathologies especially at ultra-high field strengths (≥7T). However, images acquired at these ultra-high field strengths experience substantial B_1^+ field inhomogeneities due to the shortened radiofrequency (RF) wavelengths used[5,6]. As a result, NOE_{MTR} suffers from significant signal loss in the resulting contrast images. This drop in NOE_{MTR} signal is most dramatic in the inferior regions of the brain, specifically in the mesial temporal lobe slices.

While several methods exist that attempt to correct for these B_1^+ inhomogeneities at 7T, such as post-processing algorithms or parallel transmit (pTx) techniques, they have their own sets of drawbacks and limitations[7]. One correction method that has seen a degree of success has been the use of high-permittivity aqueous dielectric padding placed near the subject's head to supplement regional low B_1^+ magnitude[8–10]. This supplemental magnetic field results from displacement currents being produced via tangential electric fields causing an increased polarization of the bulk high-permittivity materials and is described in Eq (1) below. In this expression total current density is composed of conduction (J_C) and displacement currents (J_D).

$$\nabla \times B_{1,sec} = \mu(J_C + J_D) = \mu(\sigma E + j\omega\varepsilon_o\varepsilon_r E) \quad (1)$$

The resulting spatial augmentation of the B_1^+ field has been described as a localized increase near the pads with a decrease across regions of the tissue farther away. This was suggested by Brink et al.[11] who indirectly showed that B_1^+ drop near the temporal bone in the inner ear could be increased at the cost of global head B_1^+. Dielectric pad usage and development has been extensively targeted towards neuroimaging[8,12–15], cardiac and vascular imaging[16–18], and musculoskeletal imaging[19–21] at 1.5T, 3T, and 7T field strengths.

Many metabolic imaging sequences benefit greatly from B_1^+ correction and therefore are good techniques for quantifying their influence via B_1^+ field mapping techniques. A recent study from our group showed aqueous calcium titanate padding was effective in reducing B_1^+ inhomogeneities present in glutamate-weighted CEST (GluCEST) maps at 7T located in inferior regions of the brain, such as the temporal lobes and hippocampus[22]. However,

NOE_{MTR} contrast relies primarily on a low magnitude highly homogenous B_1^+ field to generate adequate contrast, whereas GluCEST requires both high magnitude and high B_1^+ homogeneity. Therefore, the aims of this work are as follows: 1) To demonstrate the feasibility and initial reproducibility of using aqueous calcium titanate dielectric padding to correct primarily for volumetric NOE_{MTR} B_1^+ inhomogeneities in a 3D hippocampal slab of the brain and improve resulting contrast. 2) To describe the spatial augmentation behavior of the B_1^+ field across the whole brain when influenced by dielectric padding.

Methods

Dielectric Pads

Two 18×18 cm^2 dielectric pads were utilized in this work, with a composition of $CaTiO_3$ suspended in D_2O (7TNS, Multiwave Imaging, Marseille, France) having an estimated relative permittivity of 110 at 300MHz[23].

MR Image Acquisition

All images were acquired on a 7T MRI (Magnetom Terra, Siemens Healthcare, Erlangen, Germany) using a single channel transmit 32-channel receive phased array head coil (Nova Medical, Wilmington, MA, USA). Images were acquired on six healthy male subjects (ages: 23–44) after obtaining informed consent under an approved IRB protocol. Dielectric pads were placed near the temporal lobes on either side of the subject's head and due to their physical size, they extended forward to partially cover the face. Volumetric NOE_{MTR} data was acquired using a modified 3D turbo FLASH sequence, with a gradient echo readout TR = 3.5s, TE = 1.79ms, and shot TR = 6s. Each image was acquired in three shots (separate saturation/acquisition cycles) across a total scan time of approximately 10 minutes. The 3D slab was positioned in an oblique orientation in line with the hippocampus and had a thickness of 24mm (2mm per slice resolution), with an in-plane resolution of 1 × $1mm^2$ and a matrix size of 240 × 180. Magnetization preparation was achieved by using a $B_{1,\,RMS}$ pulse amplitude of 0.72μT, with a pulse length of 3s. Hanning-shaped pulses of 99 ms duration with 1ms inter-pulse delay were applied at offset frequencies from −5 to 5ppm in step sizes of 0.2ppm relative to water proton resonance frequency, along with 100ppm saturation offset. Additionally, whole brain B_1^+ field maps were acquired on a single subject under the same dielectric padding conditions with an isotropic resolution of 2mm. Subsequently, these whole brain B_1 maps were then used to generate difference maps across the whole brain volume by subtracting the data taken with no pads from that taken with pads.

Analysis and Post-processing

The acquired −3.5ppm NOE signal was subtracted from and normalized to the 100ppm signal to account for the large confounding amide signal present at 3.5ppm. This can be seen in Eq (2) below where S_0 is the intensity of the signal from the saturation pulse applied at 100ppm.

$$NOE_{MTR} = \frac{S_0 - S(-3.5ppm)}{S_0} \times 100 \quad (2)$$

It should be noted that while this quantity can measure relative changes, it shows an aggregate effect of NOE, magnetization transfer (MT), and direct saturation (DS). The resulting NOE_{MTR} images were corrected for B_0 inhomogeneities using WASSR acquisition acquired at offsets frequencies ranging from 0 to ±1ppm in step sizes of 0.1ppm[24] and B_1 field maps were generated as in Volz et al.[25]. An additional linear B_1^+ post-processing correction step was also applied separately to the acquired NOE_{MTR} images after B_0 correction via local interpolation to a second order polynoimal[26]. To assess the efficacy of dielectric pads on specific brain regions, the NOE_{MTR} contrast images were segmented between gray and white matter as well as various bilateral sub-cortical regions such as the thalamus, hippocampus, and amygdala. Linear mixed effect models were performed in the R statistical environment to estimate the effect of dielectric padding on the changes in relative B_1^+ and NOE_{MTR} contrast. Image post-processing was performed using MATLAB (The Mathworks Inc., Natick, MA, USA) and SPM12[27], cortical and sub-cortical tissue segmentation was performed using HD-BET[28], FSL[29], and ANTS[30].

Results

Transmit efficiency maps seen in Figure 1, show that when pads were present the values in the temporal lobes increased while posterior region values decreased compared to maps acquired without padding present, reflecting a net increase in homogeneity within the image slab. This change in B_1^+ between pad conditions is further emphasized by the corresponding transmit efficiency difference maps which show a clear and consistent increase in the temporal lobe regions and decrease in the posterior regions. However, results showed no statistically significant differences present in transmit efficiency values ($p = 0.25$) between padding conditions. It should be noted that this lack of significance most likely reflects the minimal change in mean B_1^+ while not considering the increase in overall homogeneity across the slab. These results are summarized in Table 1 showing mean and standard deviation values. These values show approximately the same mean transmit efficiency value, 0.048, for both pad conditions. However, a reduction in standard deviation with pads was seen, 0.011, compared to no pads present, 0.013.

Corresponding uncorrected NOE_{MTR} contrast images utilizing pads reflect this change in B_1^+ in the form of increased contrast in the temporal lobes and was consistently increased across all six subjects, as seen in Figure 2. The images without linear post-processing in the upper half of Figure 2 showed a statistically significant difference ($p < 0.001$) between padding conditions. A separate linear correction was applied to these same NOE_{MTR} images, seen in the bottom half of Figure 2, and show the same contrast enhancement in the temporal lobe regions as well as additional overall enhancement in the posterior regions of the brain when pads were used. These linear corrected results also produced a statistically significant difference ($p < 0.001$) between padding conditions. This is further supported by box plots in Figure 3, showing the variability for each individual subject between pad and post-processing conditions averaged over all slices. Consistently seen across all subjects',

pads, and linear correction alone each generally increased NOE_{MTR} contrast while also reducing the NOE_{MTR} variability. The highest amount of contrast and lowest amount of variability was achieved when both methods were applied together. More general histograms showing contrast changes between experimental conditions can be viewed in the supporting information as figure S1.

The NOE_{MTR} data shown in Table 1 here shows a highly consistent convergence in NOE_{MTR} contrast values across all subjects towards approximately 22.3% mean for the non-linear corrected pad data compared to 19.5% with no pads. Similarly, a reduction in standard deviation was also seen with pads, 7.5%, compared to no pads present, 9.1%. This same trend was also seen for linear corrected data where the same convergence in NOE_{MTR} values was seen towards approximately 31.2% with pads compared to 26.9% with no pads. Standard deviations saw the same trend with a reduction observed with pads, 8.9%, compared to no pads, 10.3%.

Figure 4 shows a full linear corrected NOE_{MTR} acquisition from one subject (except for the first and last slices due to phasing artifacts being present) showing, in detail, the differences in contrast between pad conditions across the entire 3D slab. In these images the pads had a substantial corrective effect not only in the temporal lobe regions but also in the posterior regions of the brain as well. In addition, the effect of the pads can be consistently seen across all slices with a slight diminishment in the inferior slices. In the segmented subcortical regions, an increase in mean linear corrected NOE_{MTR} contrast values were consistently observed when pads were used. These segmented regions and their corresponding histograms can be viewed in the supporting information as figures S2 and S3.

Discussion

In this work, calcium titanate dielectric pads were utilized in improving B_1^+ inhomogeneities present in 7T NOE_{MTR} images and improving resulting contrast. Feasibility and initial reproducibility were shown by acquiring 3D hippocampal slab data across six healthy subjects with and without pads placed on either side of the head near the temporal lobes. The transmit efficiency maps acquired across the hippocampal slab show a substantial change not only in the temporal lobes but also in the posterior regions. This matches initial hypotheses on pad function by Teeuwisse et al.[23] who described when using pads, a local B_1^+ increase is expected while globally it will decrease.

When viewing the NOE_{MTR} images, dielectric pads showed a high degree of contrast enhancement across all six subjects with and without linear post-processing correction. The pads were not only able to improve the mean NOE_{MTR} values within a single subject but also equalized the means between subjects towards a nominal value of approximately 22% without linear correction and 30% with linear correction. The linear correction applied to the no pad data provided some corrective effect but was unable to substantially improve the NOE_{MTR} contrast values in the temporal lobes and additionally amplified the noise in those low B_1^+ regions.

The variability of these correction methods for all subjects individually, where data absent of pads or linear correction, showed the largest amount of NOE_{MTR} variability along with the lowest mean value. Incorporating the pads or linear post-processing separately showed a relatively consistent improvement in both areas by increasing the mean contrast and decreasing the variability. However, incorporating both to each subject's data showed a greater improvement than either alone could achieve, illustrated in the consistently high NOE_{MTR} values and low variability. This supports the notion that a multi-corrective approach is needed to adequately improve inhomogeneities and resulting contrast without leading to worse quality within low B_1^+ regions. With the inferior slices of the acquired slab experiencing more inhomogeneities than the superior ones, evaluating the corrective effect on the whole slab on a per slice basis was also of interest. This is illustrated by showing that slice 2 saw almost just as much contrast enhancement compared to slice 11 in the complete subject acquisition presented.

Tissue specific analysis also showed that both gray and white matter saw an increase in NOE_{MTR} with gray matter seeing the larger increase. With a larger fraction of gray matter being positioned physically closer to the pads during acquisition, this increase in contrast is expected. All sub-cortical linear corrected NOE_{MTR} values also saw an increase when pads were used versus absent. This reflects that not only does superficial gray matter benefit from pad usage but also that deep gray matter structures (such as the thalamus, hippocampus, and amygdala) also can see a substantial amount of enhancement.

While corrective effects were seen consistently across the 20mm slab of the main NOE_{MTR} acquisition region, dielectric pads augment the B_1^+ fields across the entirety of the brain. An additional aim of this work also sought to show the augmentation of the spatial B_1^+ field distribution across the whole brain. Volumetric difference maps show regions of both increasing and decreasing relative B_1^+ strength across the entire brain when dielectric pads were placed on either side of the head. Rupprecht et al.[31] previously performed numerical calculations to show that in the presence of a high permittivity material, an increased amount of coil flux density inside the bulk material caused a decrease in magnitude outside the vicinity of the material. Furthermore, this flux "focusing" effect was observed to increase with the increasing volume of material. The full volumetric B_1^+ field data render can show this more clearly as it would be expected that the most B_1^+ flux is focused through the pad material onto the temporal lobes where the pads were placed. Moving posteriorly and superiorly away from the maximum B_1^+ enhancement location, the positive increase begins to fall off and is exchanged for a decrease in B_1^+, as would be expected considering there would be less flux traveling through those regions. An example of this whole brain volumetric rendering can be viewed in the supporting information as figure S4.

In this work, NOE_{MTR} images were only acquired across a limited 20mm slab and while the change in whole brain B_1^+ could be investigated, change in whole brain NOE_{MTR} could not be due to current sequence limitations. With further sequence optimization, future work should aim to incorporate acquisitions across the entire brain to characterize pad behavior not only on B_1^+ maps but also on resulting contrast images of interest. Additionally, this work did not track changes in SAR with and without dielectric pads. Previous studies have found that pad usage not only improved resulting image contrast but also lead to decreases

in SAR levels[16,21]. Future work should also incorporate standard quantification of these changes especially for the benefit of SAR-limited sequences such as GluCEST.

In recent years, 7T has seen massive advancements in technical developments and clinical utility, especially in neurodegenerative disease diagnostics, with one of the biggest limitations, however, still being B_1^+ inhomogeneity. The most popular avenue of correcting NOE_{MTR} images (and many others) is offline post-processing, However, these correction techniques rely on B_1 dependent contrast data which may or may not be available at the B_1-powers used in vivo, particularly in certain CEST-based techniques due to SAR limitations. Furthermore, it was also seen in this work and previous work[22,32] that post-processing does not fully correct image regions that have particularly low B_1^+ values. Conversely, dielectric pads can bring regions of considerably low contrast into a more correctable regime. Therefore, multifaceted correction techniques which combine post-processing and pad usage and, even in the future, pTx, and artificial intelligence (AI) should be considered. Consideration should also be given to using dielectric pads and other methods to correct for the same B_1^+ inhomogeneities present in similar sequences at 7T such as creatine CEST (CrCEST)[33] and transient NOE (tNOE)[34].

Conclusion

The work described here demonstrates that high permittivity dielectric padding can be used to improve 7T NOE_{MTR} contrast, with and without linear correction, particularly in the temporal lobes and in several subcortical regions. With dielectric pads being historically used in correcting for B_1^+ inhomogeneities associated with anatomical images, this work represents the first use of dielectric pads with the specific goal of improving NOE_{MTR} contrast images. Acquired whole brain B_1^+ maps were also able to not only show the expected B_1^+ increases in the temporal lobes but also decreases in the posterior and superior regions of the brain, which contributed significantly to the NOE_{MTR} contrast enhancement.

Supplementary Material

Refer to Web version on PubMed Central for supplementary material.

Acknowledgments

Research reported in this work was supported by the National Institute of Biomedical Imaging and Bioengineering of the National Institutes of Health under award number P41EB029460 and by the National Institute of Aging of the National Institutes of Health under Award Numbers R01AG071725, R01AG063896, and R56AG062665.

References:

1. Liu GS, Song XL, Chan KWY, McMahon MT. Nuts and bolts of chemical exchange saturation transfer MRI. Nmr in Biomedicine. Jul 2013;26(7):810–828. doi:10.1002/nbm.2899 [PubMed: 23303716]
2. Jones CK, Huang A, Xu JD, et al. Nuclear Overhauser enhancement (NOE) imaging in the human brain at 7 T. Neuroimage. Aug 15 2013;77:114–124. doi:10.1016/j.neuroimage.2013.03.047 [PubMed: 23567889]

3. Mennecke A, Khakzar KM, German A, et al. 7 tricks for 7 T CEST: Improving the reproducibility of multipool evaluation provides insights into the effects of age and the early stages of Parkinson's disease. Nmr in Biomedicine. Mar 17 2022;doi:ARTN e4717 10.1002/nbm.4717
4. Chen L, Wei ZL, Chan KWY, et al. Protein aggregation linked to Alzheimer's disease revealed by saturation transfer MRI. Neuroimage. Mar 2019;188:380–390. doi:10.1016/j.neuroimage.2018.12.018 [PubMed: 30553917]
5. Rutland JW, Delman BN, Gill CM, Zhu C, Shrivastava RK, Balchandani P. Emerging use of ultra-high-field 7T MRI in the study of intracranial vascularity: State of the field and future directions. American Journal of Neuroradiology 2020. p. 2–9.
6. Ladd ME, Bachert P, Meyerspeer M, et al. Pros and cons of ultra-high-field MRI/MRS for human application. Prog Nucl Magn Reson Spectrosc. Dec 2018;109:1–50. doi:10.1016/j.pnmrs.2018.06.001 [PubMed: 30527132]
7. Padormo F, Beqiri A, Hajnal JV, Malik SJ. Parallel transmission for ultrahigh-field imaging. NMR Biomed. Sep 2016;29(9):1145–61. doi:10.1002/nbm.3313 [PubMed: 25989904]
8. Haines K, Smith NB, Webb AG. New high dielectric constant materials for tailoring the B1+ distribution at high magnetic fields. J Magn Reson. Apr 2010;203(2):323–7. doi:10.1016/j.jmr.2010.01.003 [PubMed: 20122862]
9. Webb AG. Dielectric materials in magnetic resonance. Concepts in Magnetic Resonance Part A. 2011;38A(4):148–184. doi:10.1002/cmr.a.20219
10. Webb A, Shchelokova A, Slobozhanyuk A, Zivkovic I, Schmidt R. Novel materials in magnetic resonance imaging: high permittivity ceramics, metamaterials, metasurfaces and artificial dielectrics. Magn Reson Mater Phy. Dec 2022;35(6):875–894. doi:10.1007/s10334-022-01007-5
11. Brink WM, van der Jagt AM, Versluis MJ, Verbist BM, Webb AG. High permittivity dielectric pads improve high spatial resolution magnetic resonance imaging of the inner ear at 7 T. Invest Radiol. May 2014;49(5):271–7. doi:10.1097/RLI.0000000000000026 [PubMed: 24566290]
12. Alsop DC, Connick TJ, Mizsei G. A spiral volume coil for improved RF field homogeneity at high static magnetic field strength. Magn Reson Med. Jul 1998;40(1):49–54. doi:10.1002/mrm.1910400107 [PubMed: 9660552]
13. Yang QX, Mao W, Wang J, et al. Manipulation of image intensity distribution at 7.0 T: passive RF shimming and focusing with dielectric materials. J Magn Reson Imaging. Jul 2006;24(1):197–202. doi:10.1002/jmri.20603 [PubMed: 16755543]
14. Sica CT, Rupprecht S, Hou RJ, et al. Toward whole-cortex enhancement with an ultrahigh dielectric constant helmet at 3T. Magn Reson Med. Mar 2020;83(3):1123–1134. doi:10.1002/mrm.27962 [PubMed: 31502708]
15. O'Reilly TPA, Webb AG, Brink WM. Practical improvements in the design of high permittivity pads for dielectric shimming in neuroimaging at 7T. J Magn Reson. Sep 2016;270:108–114. doi:10.1016/j.jmr.2016.07.003 [PubMed: 27434779]
16. Brink WM, Webb AG. High permittivity pads reduce specific absorption rate, improve B1 homogeneity, and increase contrast-to-noise ratio for functional cardiac MRI at 3 T. Magn Reson Med. Apr 2014;71(4):1632–40. doi:10.1002/mrm.24778 [PubMed: 23661547]
17. de Heer P, Bizino MB, Versluis MJ, Webb AG, Lamb HJ. Improved Cardiac Proton Magnetic Resonance Spectroscopy at 3 T Using High Permittivity Pads. Invest Radiol. Feb 2016;51(2):134–8. doi:10.1097/RLI.0000000000000214 [PubMed: 26447495]
18. Lindley MD, Kim D, Morrell G, et al. High-permittivity thin dielectric padding improves fresh blood imaging of femoral arteries at 3 T. Invest Radiol. Feb 2015;50(2):101–7. doi:10.1097/RLI.0000000000000106 [PubMed: 25329606]
19. Zivkovic I, Teeuwisse W, Slobozhanyuk A, Nenasheva E, Webb A. High permittivity ceramics improve the transmit field and receive efficiency of a commercial extremity coil at 1.5 Tesla. Journal of Magnetic Resonance: The Authors; 2019. p. 59–65.
20. Fagan AJ, Welker KM, Amrami KK, et al. Image Artifact Management for Clinical Magnetic Resonance Imaging on a 7 T Scanner Using Single-Channel Radiofrequency Transmit Mode. Invest Radiol. Dec 2019;54(12):781–791. doi:10.1097/RLI.0000000000000598 [PubMed: 31503079]

21. Koolstra K, Börnert P, Brink W, Webb A. Improved image quality and reduced power deposition in the spine at 3 T using extremely high permittivity materials. Magnetic Resonance in Medicine 2018. p. 1192–1199. [PubMed: 28543615]
22. Jacobs PS, Benyard B, Cember A, et al. Repeatability of B-1(+) inhomogeneity correction of volumetric (3D) glutamate CEST via High-permittivity dielectric padding at 7T. Magnetic Resonance in Medicine. Aug 15 2022;doi:10.1002/mrm.29409
23. Teeuwisse WM, Brink WM, Webb AG. Quantitative assessment of the effects of high-permittivity pads in 7 Tesla MRI of the brain. Magn Reson Med. May 2012;67(5):1285–93. doi:10.1002/mrm.23108 [PubMed: 21826732]
24. Kim M, Gillen J, Landman BA, Zhou J, van Zijl PC. Water saturation shift referencing (WASSR) for chemical exchange saturation transfer (CEST) experiments. Magn Reson Med. Jun 2009;61(6):1441–50. doi:10.1002/mrm.21873 [PubMed: 19358232]
25. Volz S, Noth U, Rotarska-Jagiela A, Deichmann R. A fast B1-mapping method for the correction and normalization of magnetization transfer ratio maps at 3 T. Neuroimage. Feb 15 2010;49(4):3015–26. doi:10.1016/j.neuroimage.2009.11.054 [PubMed: 19948229]
26. Windschuh J, Zaiss M, Meissner JE, et al. Correction of B1-inhomogeneities for relaxation-compensated CEST imaging at 7T. Nmr in Biomedicine. May 2015;28(5):529–537. doi:10.1002/nbm.3283 [PubMed: 25788155]
27. Friston KJ. Statistical parametric mapping : the analysis of funtional brain images. 1st ed. Elsevier/Academic Press; 2007:vii, 647 p.
28. Isensee F, Schell M, Pflueger I, et al. Automated brain extraction of multisequence MRI using artificial neural networks. Hum Brain Mapp. Dec 1 2019;40(17):4952–4964. doi:10.1002/hbm.24750 [PubMed: 31403237]
29. Jenkinson M, Beckmann CF, Behrens TE, Woolrich MW, Smith SM. Fsl. Neuroimage. Aug 15 2012;62(2):782–90. doi:10.1016/j.neuroimage.2011.09.015 [PubMed: 21979382]
30. Avants BB, Tustison N, Song G. Advanced normalization tools (ANTS). Insight j. 2009;2(365):1–35.
31. Rupprecht S, Sica CT, Chen W, Lanagan MT, Yang QX. Improvements of transmit efficiency and receive sensitivity with ultrahigh dielectric constant (uHDC) ceramics at 1.5 T and 3 T. Magnetic Resonance in Medicine. May 2018;79(5):2842–2851. doi:10.1002/mrm.26943 [PubMed: 28948637]
32. Cember ATJ, Hariharan H, Kumar D, Nanga RPR, Reddy R. Improved method for post-processing correction of B1 inhomogeneity in glutamate-weighted CEST images of the human brain. NMR Biomed. Jun 2021;34(6):e4503. doi:10.1002/nbm.4503 [PubMed: 33749037]
33. Singh A, Debnath A, Cai K, et al. Evaluating the feasibility of creatine-weighted CEST MRI in human brain at 7 T using a Z-spectral fitting approach. NMR Biomed. Dec 2019;32(12):e4176. doi:10.1002/nbm.4176 [PubMed: 31608510]
34. Kumar D, Benyard B, Soni ND, Swain A, Wilson N, Reddy R. Feasibility of transient nuclear Overhauser effect imaging in brain at 7 T. Magn Reson Med. Apr 2023;89(4):1357–1367. doi:10.1002/mrm.29519 [PubMed: 36372994]

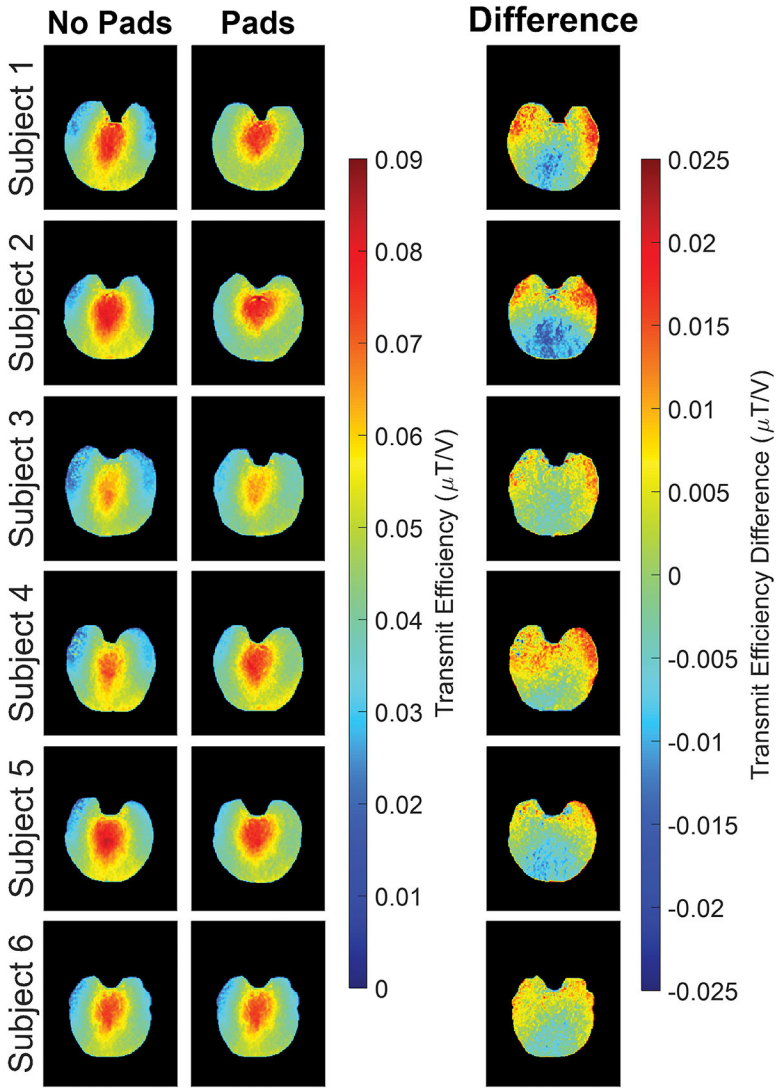

Figure 1.

Acquired transmit efficiency maps shown for all six subjects with and without dielectric padding for a hippocampal slice. Data acquired with dielectric pads present shows an increase in homogeneity in the temporal lobes and posterior region of the brain compared to those acquired without. Generated transmit efficiency difference maps can also be seen for each subject emphasizing the differences.

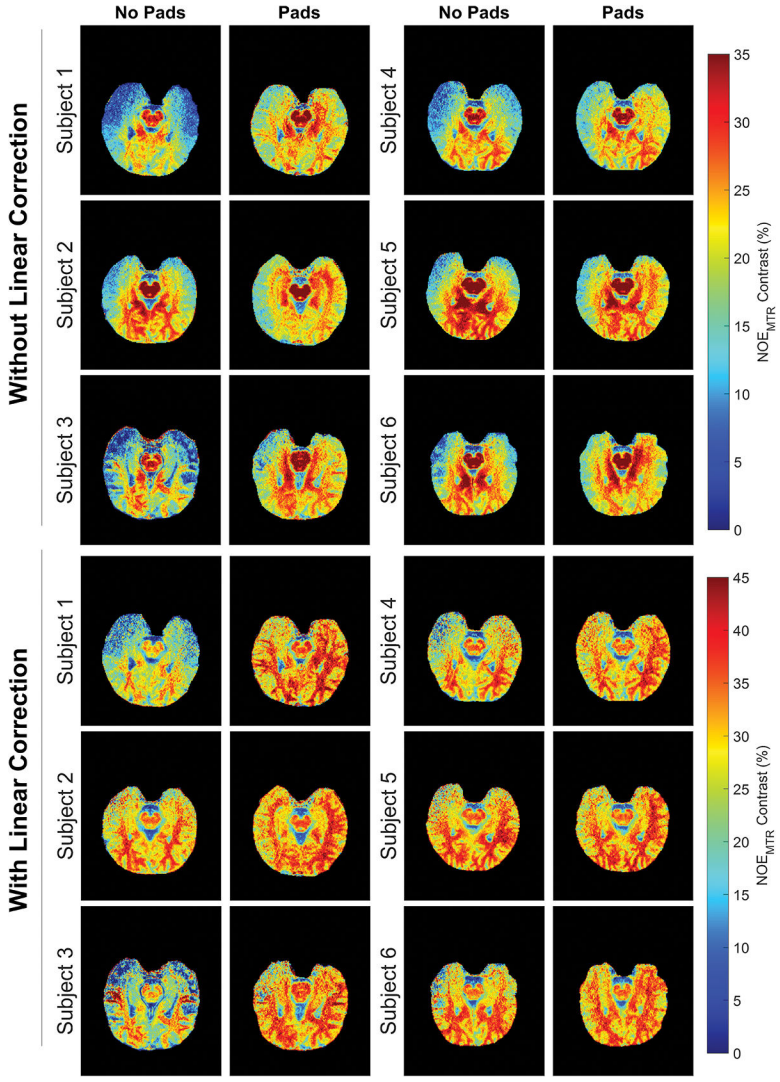

Figure 2.

NOE_{MTR} images acquired across all six subjects with and without dielectric pads, between post-processing conditions. The images seen in the upper half have not had post-processing applied to them while the images in the bottom half have had this correction applied. Images acquired with only dielectric padding show a substantial increase in contrast in the temporal lobe and posterior regions compared to those acquired without padding. When linear correction is incorporated the amount of contrast enhancement is further increased.

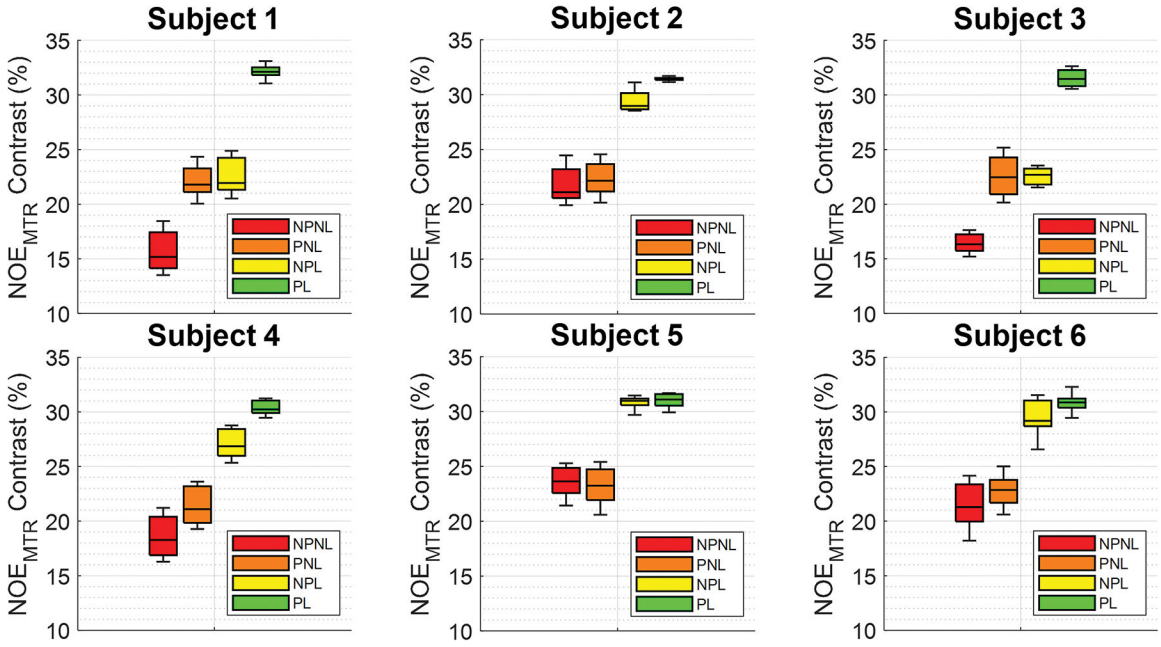

Figure 3.

Boxplots showing summary for each subject across the experimental conditions. The labelled conditions seen here are as follows: No pads without linear correction (NPNL), pads without linear correction (PNL), no pads with linear correction (NPL), and pads with linear correction (PL). Pads and linear correction alone generally increase NOE_{MTR} contrast while reducing variability, while applying both together achieve the highest contrast and lowest contrast variability.

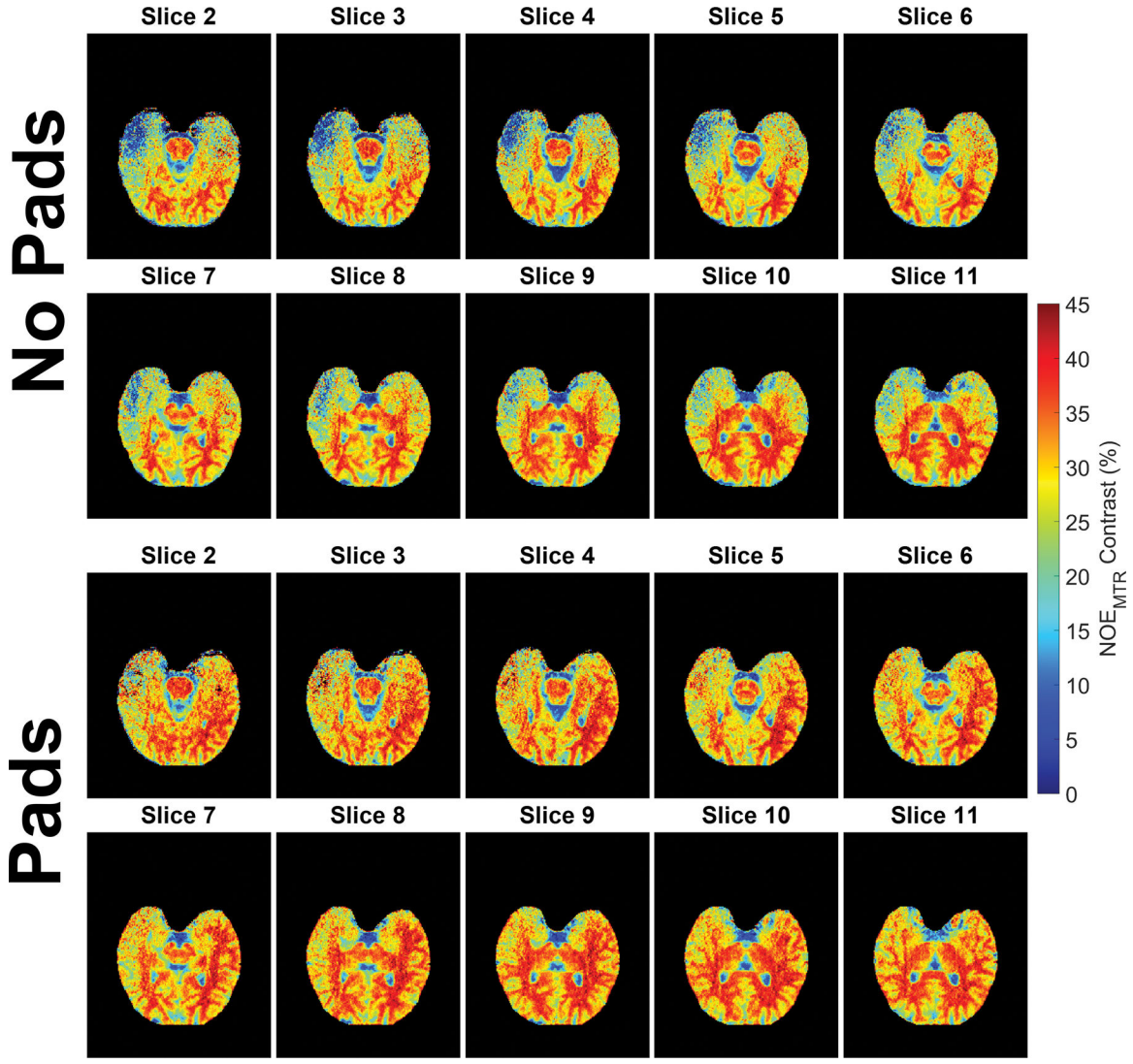

Figure 4.

A same subject whole slab comparison of linear corrected NOE_{MTR} images between padding conditions. In this data, slice 2 corresponds to more inferior regions of the slab while slice 11 is 20mm higher. Dielectric padding substantially increased NOE_{MTR} contrast not only in the temporal lobe region but also in the posterior regions of the brain as well. The first and last slices were omitted due to the presence of phasing artifacts.

Table 1.

Calculated mean and standard deviation values for transmit efficiency and NOE_{MTR} contrast images with and without linear correction across all subjects and padding conditions. All values were calculated across the entire 3D slab excluding the first and last slices.

		Transmit Efficiency (μT/V)	NOE_{MTR} Contrast (%) (No Linear Correction)	NOE_{MTR} Contrast (%) (Linear Correction)
No Pads	Subject 1	0.049 (0.013)	15.63 (8.55)	22.54 (10.53)
	Subject 2	0.051 (0.014)	21.72 (8.42)	29.39 (9.52)
	Subject 3	0.043 (0.012)	16.37 (12.42)	22.58 (14.18)
	Subject 4	0.048 (0.013)	18.53 (8.26)	27.02 (9.73)
	Subject 5	0.050 (0.014)	23.54 (8.49)	30.82 (7.85)
	Subject 6	0.048 (0.013)	21.35 (8.82)	29.37 (9.67)
	Total	**0.048 (0.013)**	**19.52 (9.16)**	**26.95 (10.38)**
Pads	Subject 1	0.050 (0.010)	22.02 (8.54)	32.15 (10.51)
	Subject 2	0.048 (0.012)	22.29 (6.99)	31.44 (8.77)
	Subject 3	0.043 (0.009)	22.60 (8.52)	31.49 (10.33)
	Subject 4	0.048 (0.010)	21.37 (6.86)	30.36 (8.29)
	Subject 5	0.049 (0.011)	23.18 (7.56)	30.98 (7.91)
	Subject 6	0.048 (0.011)	22.72 (7.00)	30.84 (8.17)
	Total	**0.048 (0.011)**	**22.36 (7.57)**	**31.21 (8.99)**